



ELSEVIER

Available online at www.sciencedirect.com

SCIENCE @ DIRECT®

Nuclear Instruments and Methods in Physics Research A ■ (■■■■) ■■■-■■■

**NUCLEAR
INSTRUMENTS
& METHODS
IN PHYSICS
RESEARCH**
Section Awww.elsevier.com/locate/nima

Complete tests of 2000 Hamamatsu R7525HA phototubes for the CMS-HF Forward Calorimeter

U. Akgun^{a,*}, A.S. Ayan^a, P. Bruecken^a, F. Duru^a, E. Gülmez^b, A. Mestvirishvili^a, M. Miller^a, J. Olson^a, Y. Onel^a, I. Schmidt^a

^a*Department of Physics and Astronomy, The University of Iowa, 203 Van Allen Hall, Iowa City, IA, 52242, USA*

^b*Physics Department, Bogazici University, Istanbul, 34342, Turkey*

Received 17 March 2005; accepted 31 March 2005

Abstract

Approximately 2000 PMTs will be used to detect the Cherenkov light generated in quartz fibers embedded in the CMS-HF Forward Calorimeter. The Hamamatsu R7525HA PMT was chosen for this purpose. We measured the transit time, transit time spread, pulse width, rise time, anode dark current, and relative gain for each tube in the test station at the University of Iowa. Life-time, gain versus high voltage, and single photoelectron spectrum measurements were also done on a small sample of PMTs. All the tubes were tested to verify that they conform to the HF requirements.

© 2005 Elsevier B.V. All rights reserved.

PACS: 29.40.Ka; 29.40.Vj; 29.90.+r; 85.60.Ha

Keywords: PMT; HF-calorimeter; CMS

1. Introduction

The Compact Muon Solenoid (CMS) Experiment at the Large Hadron Collider (LHC) at the European Particle Physics Laboratory CERN is equipped with a forward calorimeter (HF) that uses almost 2000 phototubes to read out Cher-

enkov light from quartz fibers. The Hamamatsu R7525HA PMT has been chosen for this purpose [1]. It is crucial to understand the parameters of these PMTs in order to optimize the operation of the HF Calorimeter. Detailed results of these measurements will also guide us in the installation of the PMTs in the calorimeter to provide smooth operation and better performance. Furthermore, individual measurements may be useful in attempting to solve possible future problems related to the PMT's.

*Corresponding author. Tel.: +319 335 3574;
fax: +319 335 1753.

E-mail address: ugur-akgun@uiowa.edu (U. Akgun).

In this study we measured the various characteristics of all the tubes that will be used in the HF Forward Calorimeter, including spares. The measurements include the transit time and its spread, pulse width, rise time, dark current, and relative gain. The results of these measurements are accumulated in a database. Absolute gain and single photo electron resolution of a small sample of tubes were also determined. The characteristic lifetime of these tubes was estimated by exposing two PMTs to continuous light. This report explains the testing procedure and displays the results of the measurements.

2. The CMS-HF Forward Calorimeter

The CMS-HF Forward Calorimeter design allows it to be efficient over a pseudorapidity (η) range of $3 < \eta < 5$. This pseudorapidity region is especially important for heavy higgs and SUSY searches. Additional help from the HF calorimeter for these searches would be the identification of forward jets. Tagging the very forward jets would greatly help identify specific processes relevant to these particles.

The charged particles entering the HF Forward Calorimeter produce showers in the iron absorber of the calorimeter. These showers are sampled with the help of Cherenkov radiation generated in quartz fibers. Only electrons and positrons in the shower are fast enough to produce Cherenkov light, with the result that the calorimeter is mainly sensitive to the electromagnetic showers and the electromagnetic core of hadronic showers. Since slower particles and particles produced by induced radioactivity are below the Cherenkov threshold, the signal from the calorimeter is very clean and fast.

The HF Forward Calorimeter has a cylindrical shape. It is 1.65 m long and has a radius of 1.4 m. The beam pipe passes along the central cylindrical axis. The absorber is made of iron and divided into 18 wedges covering 20° . One millimeter wide holes are drilled into the wedges parallel to the beam. Six hundred micron thick plastic clad quartz fibers are inserted into these holes as the sensitive material in the calorimeter. Long (1.65 m) and short (1.43 m)

fibers alternate in the fiber matrix. Each wedge is further divided into 24 towers. The short and long fibers from a specific tower are bundled separately. Each bundle is attached to its own phototube through a 42-cm long light guide.

There are 48 PMTs per wedge and a total of 18 wedges in one HF endcap unit. This brings the total PMT's to be used in both ends of HF to 1728. Including spares, there will be 2000 tubes. The characteristics and the quality of the phototubes are closely related to the successful operation of the HF Calorimeter.

2.1. The HF requirements for PMTs

Table 1 summarizes all the requirements relevant to the mechanical design and the operation of the HF Forward Calorimeter. Furthermore, the electronics that will process the PMT signals requires low-amplitude signals. Therefore, the PMTs should be operated at a low gain but still satisfy all the timing, gain, efficiency, and resolution requirements. The Hamamatsu R7525HA PMT was chosen [1]. Quality control and a check of each tube to be used in the calorimeter is the next step, which is the subject of this report.

3. The University of Iowa CMS-HF PMT Test Station

The University of Iowa PMT Test Station was designed initially for comparison measurements and then altered for quality control measurements by the time the PMTs started to arrive from the manufacturer. The various setups are housed in three dark boxes. The dark boxes are made of plywood with the inside surfaces covered with light absorbing black cloth. An optical table forms the bottom side of the first two dark boxes. The first box houses the setup used in timing, and single photoelectron resolution measurements. The relative gain, dark current, and gain versus HV measurements are done in the second dark box. The third dark box is independent of these two and used only for the lifetime test. Each dark box has a patch panel on the side for signal and HV cables. A Tektronix Oscilloscope (TDS5104 digital

Table 1
Summary of the HF-PMT specifications

Mechanical requirements	
Window material	Borosilicate glass
Effective photocathode diameter	22–28 mm, head-on
Quantum efficiency	> 15% (400–500 nm)
Photocathode lifetime	> 200 mC
Stability	< $\pm 3\%$ within any 48 h period
Envelope	Opaque and HV conductive coating
Operational requirements	
Anode current versus position	<20% with 3 mm spot scan
Gain	10^4 – 10^5 , 10^5 at less than $0.75 \times V_{KA}$ (max)
Single photoelectron resolution	rms/mean of SPE peak 50% or better ^a
Pulse linearity	$\pm 2\%$ for 1–3000 photoelectrons
Anode pulse rise-time	<5 ns
Transit time	<25 ns preferred
Transit time spread	<2 ns preferred
Pulse width	<15 ns FWHM
Gain (1/2)-lifetime	>1500 C
Average cathode current	<1 nA ($g = 10^4$)
Average anode current	<10 μ A ($g = 10^4$)
Anode dark current	<2 nA ($g = 10^4$)

^aIn this paper, all the resolution measurements are given in terms of FWHM/peak position which yields values about 2–2.5 times larger than rms/mean method (FWHM = 2.534σ for a Gaussian).

oscilloscope with 1 GHz Bandwidth and 5 Gs/s sampling rate) is used for timing measurements. Gain and dark current measurements are done using an ADC and a nanoammeter.

4. PMT tests and their results

There are two types of tests; complete and sampling tests. Complete tests are done on all the tubes. These include the measurements on the timing response: transit time, transit time spread, pulse width, and rise time. There are also dark current, and relative gain measurements. The

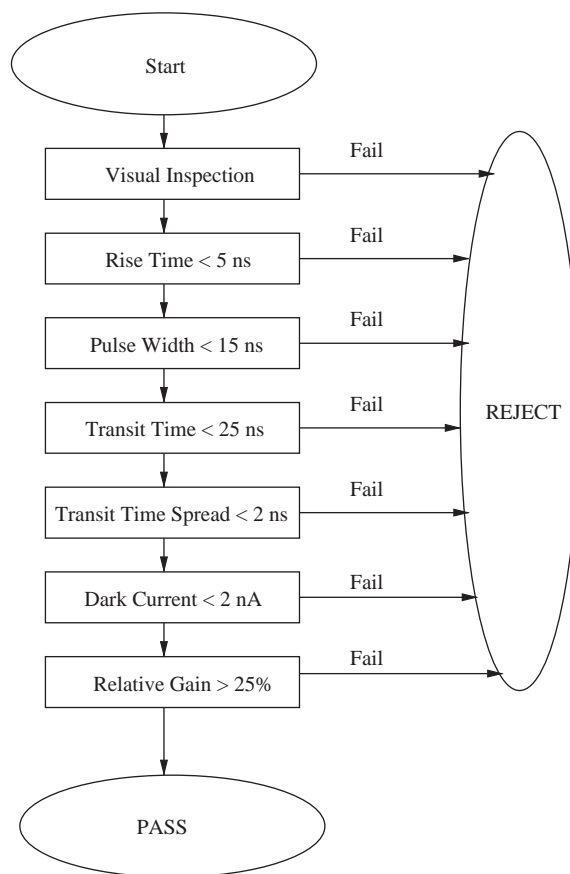


Fig. 1. Testing algorithm.

second group of tests, which are single photoelectron resolution, spatial uniformity of the photocathode surface, and gain versus HV measurements, are done only on a small sample of tubes selected randomly. The lifetime test is done only on a few PMTs since the PMT is completely burned during this test.

Each tube is logged in upon arrival and inspected visually prior to the general tests mentioned above. Any cracks, scratches, etc. are noted. The envelope is checked for HV conductive coating and opaqueness. After this the tubes are ready for testing. The algorithm of the testing procedure is displayed in Fig. 1. Our rejection limits, based on the HF requirements (Table 1), are noted in the figure also.

4.1. Complete tests

4.1.1. Timing tests

Well defined time response of the PMT's is important for the smooth operation of the calorimeter. Since successive collisions at the LHC may occur in 25 ns intervals, the resulting response pulse width should be less than this time interval. Hamamatsu R7525HA provides this kind of time response.

The setup used in timing measurements was developed during the selection [1] process and finalized for the tests (Fig. 2). In this setup, a 337 nm nitrogen pulsed laser is used as the light source. The laser light passes through a neutral density filter (NDF) and falls on a 30/70 beam splitter. The reflected light goes to a PIN diode to provide the trigger and reference signal. The transmitted light passes through more NDFs before hitting the phototube. These NDFs are used to provide appropriate attenuation levels. NDFs are placed on a wheel that is controlled through the data acquisition program. Identical cables bring the PIN diode signal and the PMT

anode signal to the oscilloscope. Since the transmitted light travels 70 cm further than the reflected light, 2.3 ns additional time delay in the transmitted light is taken into account in the analyzing program.

A standard Hamamatsu resistive base (E2624MOD) is used for the PMTs. For these tubes 1100 V gives an average gain of about 5×10^4 .

The transit time is measured as the time difference between the PIN diode and the PMT signals when both signals reach 50% of their peak values successively. The rise time is defined as the time interval when the signal increases from 10% of the peak value to 90%. (What we mention here as rise time is actually the fall time since the signal is negative.) Width is simply the FWHM of the PMT signal. All these measurements are done automatically by the oscilloscope. For the transit time, pulse width, and rise time measurements, oscilloscope takes data in the single sample mode. It acquires 100 signals and then an internal program to the oscilloscope calculates the averages. On the other hand, the transit time

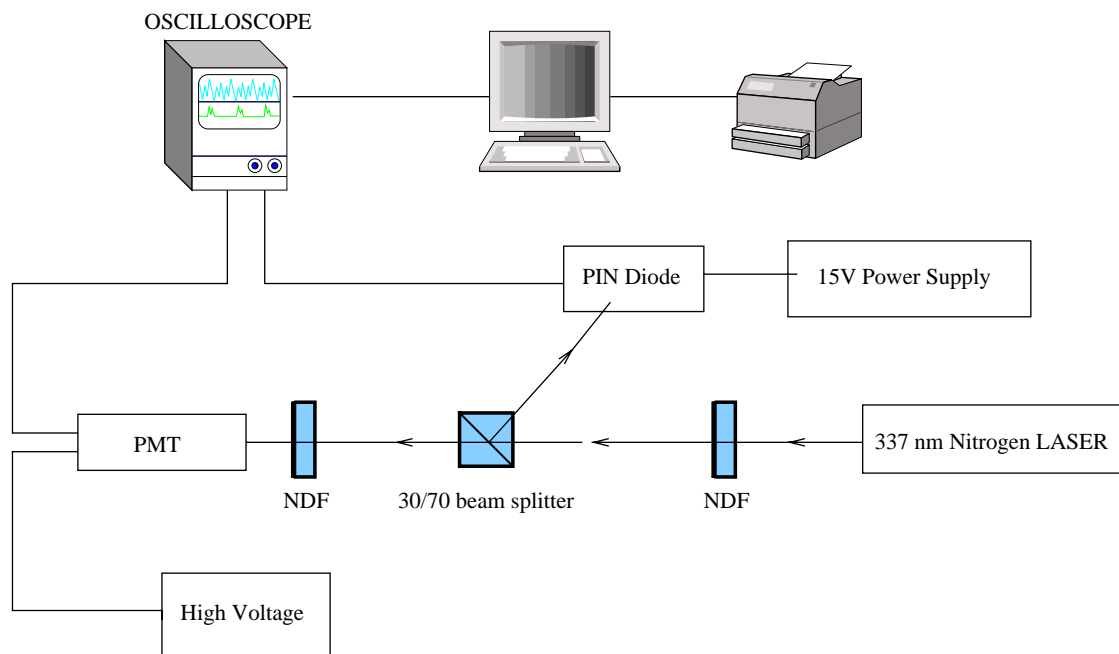


Fig. 2. Test setup for timing measurements.

spread (fluctuations in the transit time) is simply the standard deviation of the 100 transit time values.

We have performed these measurements on one tube about 50 times to estimate the statistical uncertainty. The uncertainties are; less than 0.4% for transit time, 9% for the pulse width, 8% for the rise time, and about 30% for the transit time spread.

The transit time values show a narrow distribution around 15 ns (Fig. 3—top). All the tubes have almost the same transit time. This is very good for the smooth and stable operation of the calorimeter. The transit time spread has a wider distribution (Fig. 3—bottom), but again the overall distribution width we observe can be attributed mostly to the 30% statistical uncertainty.

The rise time (Fig. 4—top) and pulse width (Fig. 4—bottom) distributions, on the other hand,

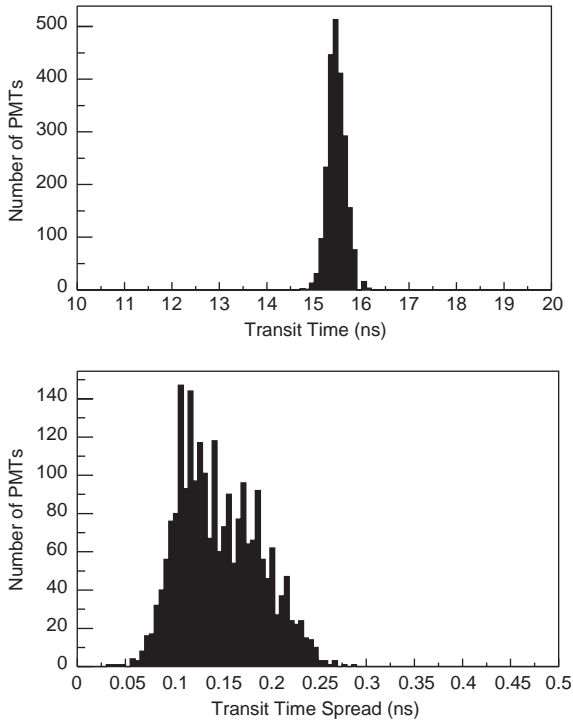


Fig. 3. Transit time (top) and transit time spread distributions (bottom) of all tested PMTs. Centroid and width values of these distributions are 15.5 ± 0.2 ns for the transit time and 0.15 ± 0.04 ns for the transit time spread.

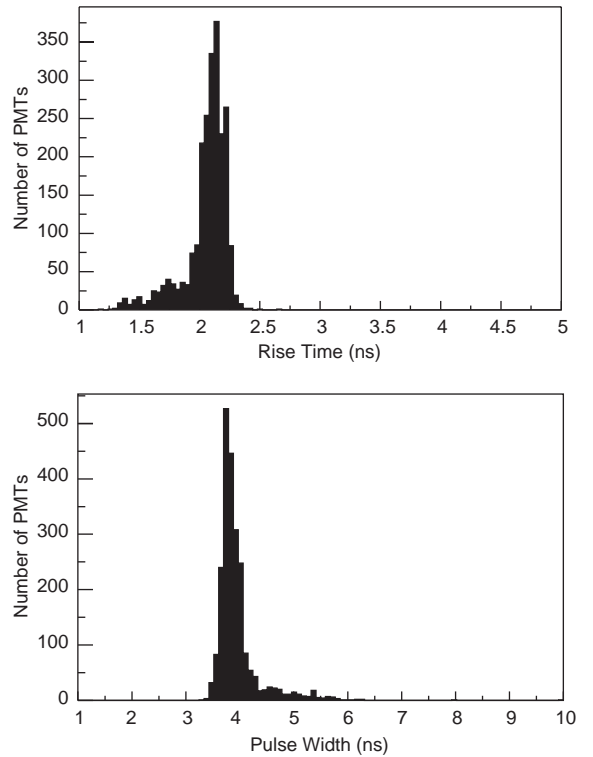


Fig. 4. Rise time (top) and pulse width (bottom) distributions for all tested PMTs. Centroid and width values (Gaussian) of these distributions are 2.1 ± 0.2 ns for the rise time and 4.0 ± 0.4 ns for the pulse width.

are somewhat wider. This could be because of our larger statistical uncertainty in these measurements. In fact, taking these larger uncertainties into account, we can also conclude that pulse width and rise time values for all the tubes are also almost the same.

4.1.2. Dark current and relative gain

The second dark box houses the dark current, relative gain, gain versus high voltage, and spatial uniformity measurement setups. In fact, a PMT-holder designed to hold eight phototubes is used in all these measurements. For both dark current and relative gains, the same reference tube (serial number CA0017) is used. The position of the reference tube is always the same. Its gain as a function of high voltage is measured several times (33 times); these measurements result in a standard deviation of about 5%. It has a gain of 6.4×10^4 at

1100 V. Its dark current at this voltage is about 0.003 nA.

A set of seven PMTs to be tested are installed in the remaining positions. High voltage for all the tubes is set to 1100 V, which is the nominal HV for 5×10^4 gain. We wait until the dark current for the reference tube reads about 0.003 nA. Then the data acquisition system reads the dark currents for all the seven tubes using a Keithley picoammeter. Ten readings at 0.5 s intervals are taken and the average of these 10 readings is recorded. If there is a reading that seems to be very high, another reading is taken after waiting for some additional time.

The dark current distribution (Fig. 5—bottom) shows that the majority of the tubes are below 0.2 nA, which is much smaller than the value (2 nA) in the HF requirements (Table 1).

After the dark current measurements, the tungsten lamp at the other end of the dark box is turned on. There is a NDF (factor = 3) and a blue filter in front of the lamp. The distance between

the lamp and the holder is 140 cm. The lamp is rated for 6 V but operated at 5 V to ensure a stable light intensity. The light intensity over all the PMT positions in the holder is almost the same within about 2%. The anode currents for all eight tubes, including the reference tube, are measured as explained above. The relative gain (with respect to the reference tube) for each tube is calculated as the ratio of the anode current for a specific tube to that for the reference tube. Relative gain defined this way is actually a combination of gain and quantum efficiency of the tube. For this reason, the histogram seen in Fig. 5—top shows a broader distribution.

The statistical uncertainties for dark current and relative gain are determined by keeping the same tube in one of the seven positions for 25 measurements. These measurements result in 8% statistical uncertainty for the dark current measurements and 4% for the relative gain measurements.

4.2. Sampling tests

The following tests take longer to perform. We have decided to do these measurements only on a sample of tubes. By studying the results of these measurements, we can understand the specific operational characteristics of the tubes better. However, we will not be using the results of these measurements to accept or reject a tube.

We use the first dark box or the timing dark box also for the single photoelectron spectrum (SPES) measurements. The detailed gain versus high-voltage measurements and horizontal and vertical scans of the photocathode surface are done in the second dark box or the relative gain dark box. In addition to these tests, we have exposed a couple of tubes in the third box to continuous light intensity to estimate the lifetime of these tubes.

4.2.1. Gain versus high voltage

The PMT gain is defined as the ratio between the anode and the cathode currents. Gain usually is a function of the dynode characteristics, number of dynodes, voltage applied on the PMT and the voltage between individual dynodes, etc. By measuring the anode and cathode currents at

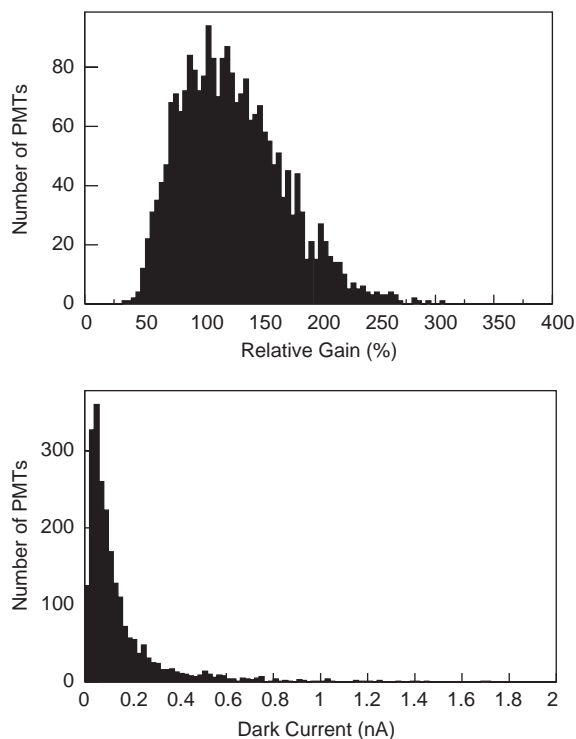


Fig. 5. Relative gain (top) and dark current distributions.

varying high voltages and then calculating the gain, we can obtain a set of gain versus high voltage values.

These measurements are performed by using two PMT holders. Each one is identical in shape but holds different bases. One has eight standard Hamamatsu bases (E2624MOD) and the other has eight simpler homemade bases for measuring the cathode current. In these homemade bases, all the dynodes and the anode are connected together, shorting the anode and all the dynodes except the first one. This way we can easily measure the cathode currents by applying the corresponding voltages between the cathode and the first dynode. For each high-voltage applied to the anode–cathode circuit there is a corresponding voltage for the cathode–first dynode circuit. These voltages can be calculated by using the voltage divider ratio of the cathode–first dynode and the cathode anode resistor circuit. Keeping the light intensity constant is important to reduce the systematic effects. To ensure the same light intensity, we apply constant voltage to the tungsten light bulb that we use and position the PMT holders identically for both types of measurements.

A histogram of gain values for over 200 PMTs (Fig. 6—top) at 1100 V shows that our nominal gain value of 5×10^4 is really the case. The histogram has a Gaussian mean value of 5.8×10^4 with a 1.8×10^4 standard deviation. This value increased for PMT's produced later compared to the tubes produced initially. In fact this is the reason for the higher average relative gain (Fig. 5—top). The relative gain as a function of time can be seen in Fig. 14.

We can also determine the relative quantum efficiencies (Fig. 6—bottom) from the relative gain measurements, since the relative gain measurement we have mentioned earlier actually is a combination of cathode efficiency and the current gain. Since the relative gain is defined as

$$\text{Relative Gain} = \frac{\text{Gain} \times \text{QE}}{\text{Gain}_{\text{ref}} \times \text{QE}_{\text{ref}}}$$

and the relative quantum efficiency as

$$\frac{\text{QE}}{\text{QE}_{\text{ref}}} = \frac{\text{Gain} \times \text{QE}}{\text{Gain}_{\text{ref}} \times \text{QE}_{\text{ref}}} \frac{\text{Gain}_{\text{ref}}}{\text{Gain}}$$

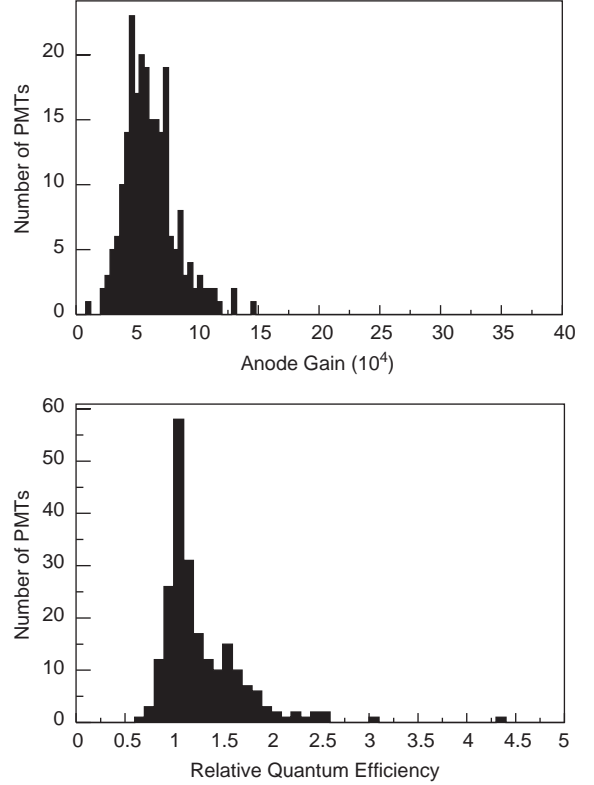


Fig. 6. Absolute gain values (top) and relative quantum efficiencies (bottom) calculated from the relative and the absolute gains. Fitting both histograms to Gaussian distributions yields $(5.8 \pm 1.8) \times 10^4$ for the absolute gains at 1100 V and 1.08 ± 0.16 for the relative quantum efficiencies.

then we can obtain the relative quantum efficiency from the relative gain and the absolute gain ratio as

$$\text{Relative QE} = \frac{\text{Relative Gain}}{\text{Absolute Gain Ratio}}$$

where

$$\text{Absolute Gain Ratio} = \frac{\text{Gain}}{\text{Gain}_{\text{ref}}}$$

The relative quantum efficiency values are mostly around 1.0 as expected because of the material used in the photocathode. Except for a few low-gain tubes, quantum efficiency versus absolute gain plot shows no correlation (Fig. 7). There seems to be some PMTs with higher quantum efficiencies (about 50% higher) and lower gains.

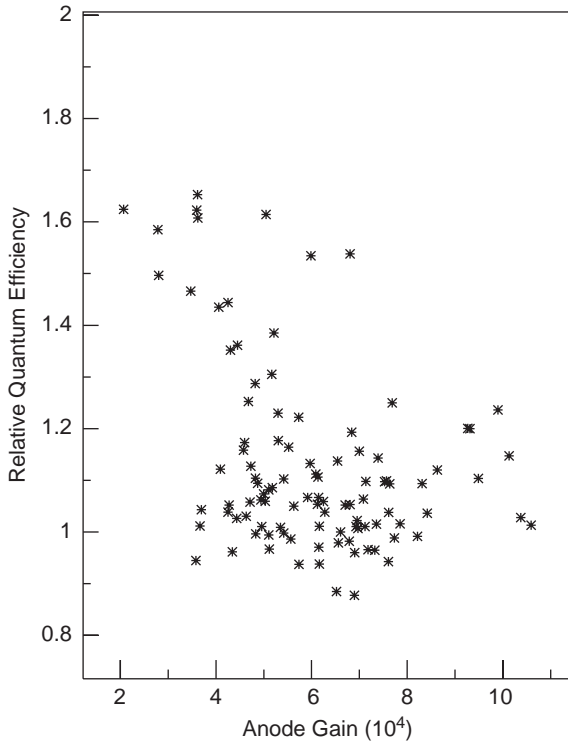


Fig. 7. There is no correlation between the absolute gains (at 1100 V for this plot) and the quantum efficiencies.

However, this combination results in relative gains around the average values.

Our absolute gain measurements are summarized in Fig. 8. Each point corresponds to the average gain at a specific HV. Error bars indicate the standard deviation for that specific measurement.

4.2.2. Spatial uniformity

Another test performed in the relative gain dark box is the horizontal and vertical scans or x - y scans. The HF requirement for the x - y uniformity is 20% with 3-mm spot scans. Spatial uniformity is initially thought to be important since 24 fibers will be bundled and read out by the same phototube. It is essential to get the same value for the same light intensity whether the light shines on one specific location on the photocathode surface or another. Otherwise, the overall energy resolution of the calorimeter will be worse.

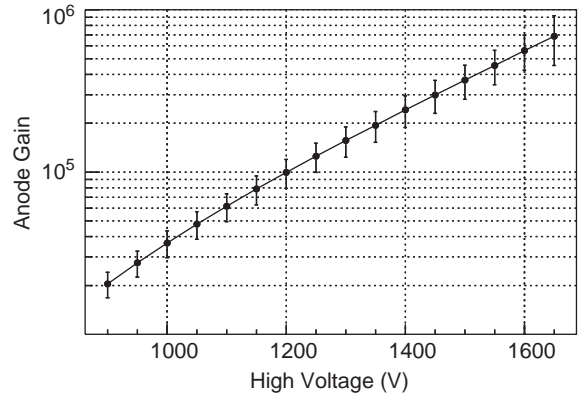


Fig. 8. Average gains at each HV value are plotted here. Standard deviation of these measurements are shown as error bars.

A single PMT is placed on the x - y scanner so that its first dynode is oriented horizontally. Our x -axis is along the first dynode and y -axis is perpendicular to that. The x - y scanner moves the tube horizontally and vertically according to the commands issued from the data acquisition program. An opaque sheet made of black kapton is placed right in front of the tube and a 3-mm diameter circular hole drilled into it. This sheet does not move. The phototube currents are integrated with the help of a LeCroy 2249A ADC. The scanner moves the tube in 1.27 mm steps at a time in both directions.

A small sample of measurements resulted in spatial nonuniformities of less than 20%, which is better than the HF requirement [2] (Fig. 9).

4.2.3. Single photoelectron spectrum (SPES)

In principle, the current gain for a PMT should be constant. However, when we look into how a PMT multiplies the photoelectrons, we see that the multiplication factor might have some uncertainty due to the statistical nature of the multiplication process.

A single photoelectron emitted from the photocathode surface will produce some number of secondary electrons from the first dynode and these will generate more electrons from the second dynode and so on, until all the electrons reach the anode. On the average a specific number of

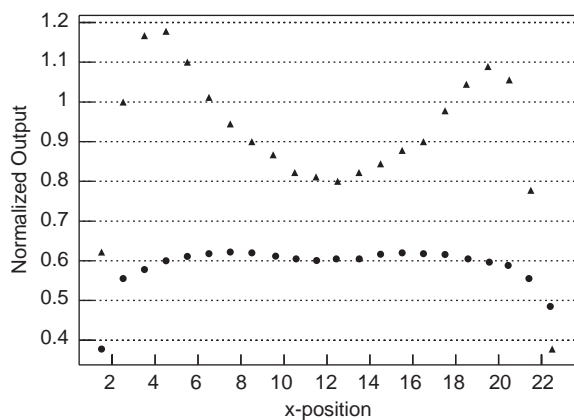


Fig. 9. Spatial uniformities as a function of position (top). Only horizontal scans are displayed here. Vertical scans produce similar results. Spatial uniformities with the light guides are also included here for comparison (bottom).

electrons are released from each dynode surface when an electron hits. However, the actual number of electrons released is not constant. It fluctuates according to the Poisson process. The total number of electrons reaching the anode shows a distribution for single photoelectrons. In case of multiple photoelectrons, the width of the distribution is related to the single photoelectron width. So the better the single photoelectron resolution is, the better the overall phototube resolution will be. To achieve a good energy resolution for the calorimeter, it is important to use phototubes with good single photoelectron resolutions.

HF requirements have a 50% or better resolution defined in terms of rms/centroid which corresponds to roughly about 125% in terms of the FWHM/peak position since $\text{FWHM} = 2.534\sigma$

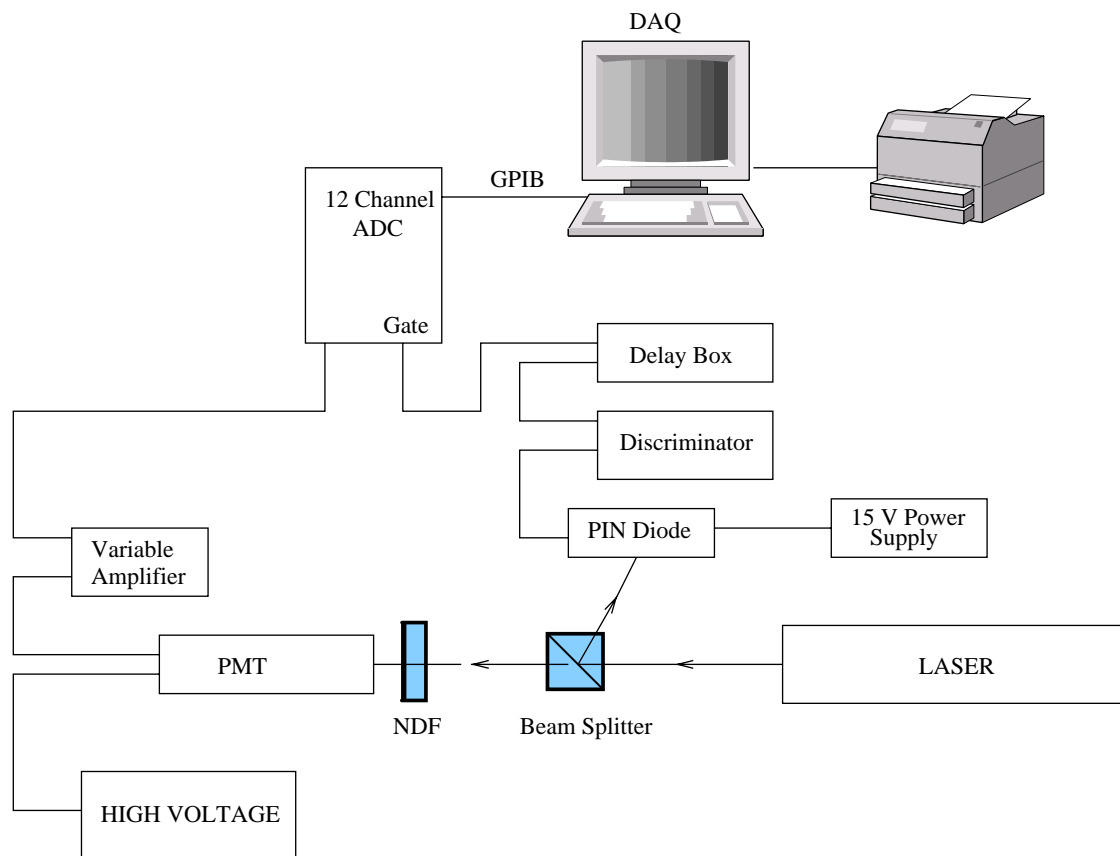


Fig. 10. Block diagram of the setup for single photoelectron spectrum measurements with ADC.

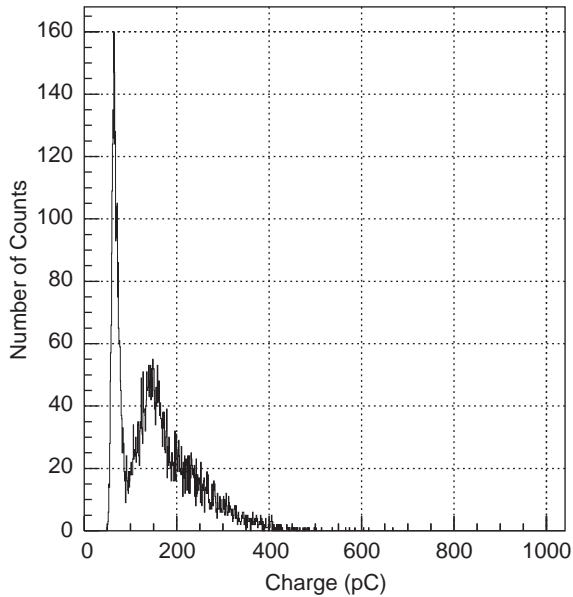


Fig. 11. Single photoelectron spectrum of Hamamatsu R7525HA at a gain of 10^4 . This specific tube has a resolution of 56%.

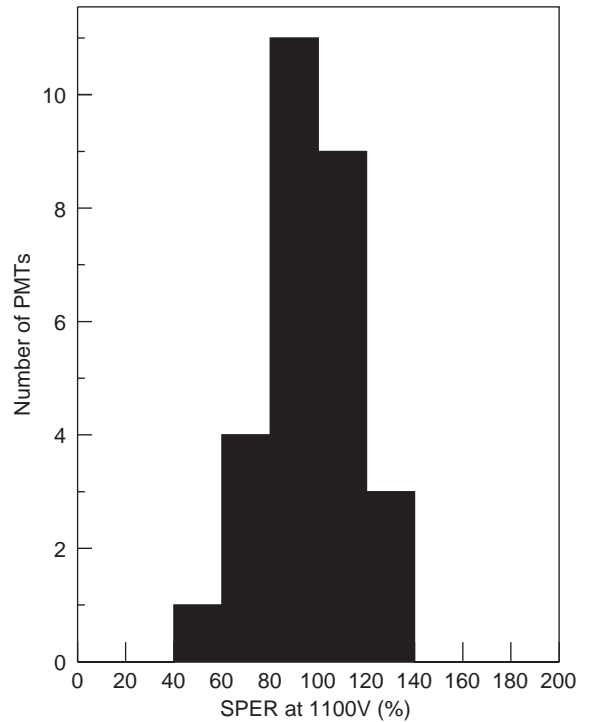


Fig. 12. Single photoelectron resolution distribution for 28 PMTs. Resolutions (SPER) are calculated as FWHM/peak position. (100% here corresponds to about 40% in terms of rms/centroid.)

for a Gaussian. We will be using the FWHM/peak position ratio in our measurements.

Single photoelectron spectra are accumulated by using almost the same setup that is used in the timing measurements (see Fig. 10). Details are given in Ref. [1]. Fig. 11 shows a sample SPES obtained with the setup displayed in Fig. 10. This specific spectrum has a 56% resolution.

Single photoelectron spectra of 28 PMTs at 1100 V are produced and their corresponding resolutions (SPER) are determined. From this set, we get a mean resolution (SPER) of 96% with a standard deviation of 19% (20% of the mean). The histogram of the distribution can be seen in Fig. 12. These results show that the single photoelectron resolution of most of the PMTs that we will be using are within the HF requirements.

4.2.4. Lifetime test

CMS will be operating 10 years and longer. During this whole period, every element in the detector should continue to operate within the parameters defined in the specific requirements for

that part. However, the PMTs will start to degrade after a while and eventually their performance will not be within their specifications. To measure the lifetime of a PMT, which is defined in terms of the accumulated charge collected from the anode when the tube gain drops to half value, we ran two PMTs at an accelerated aging rate by shining higher intensity continuous light.

The setup in the third dark box consists of a tungsten bulb as the light source and a power meter to monitor the light intensity. Phototubes are placed in the dark box and the tungsten light illuminates them. There is a NDF and a blue filter in front of the tungsten bulb. The high voltage on the tubes is adjusted a few times to give us a nominal gain of 5×10^4 while staying below the maximum anode current of $200 \mu\text{A}$. Light intensity and phototube currents are recorded in 24 h periods. This measurement took 15 months to complete.

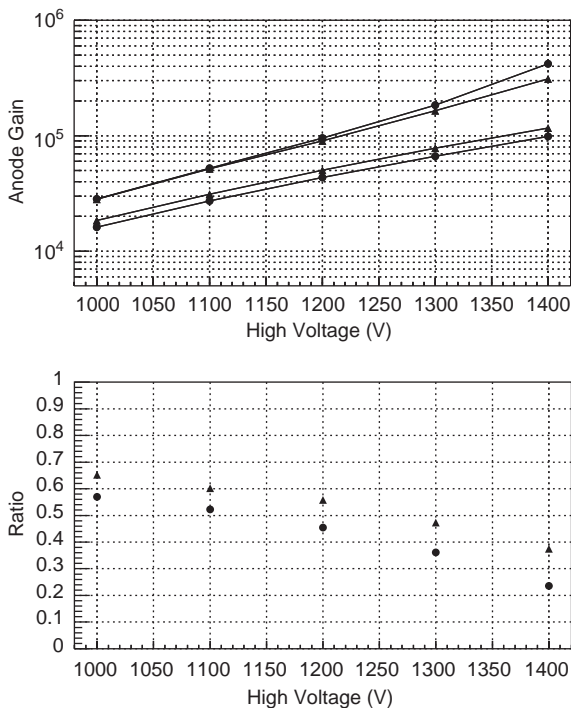


Fig. 13. Absolute gains as a function of HV are displayed before (upper curves) and after 3000 C of charge collection (lower curves) in the top portion. Bottom plot shows the relative drop in the gain as a function of HV. Triangles are for the PMT (serial no: CA0252) with 3000 C and circles for the PMT (serial no: CA0472) with 3250 C.

After about 1100 and 3000 C of charge collection, the PMT characteristics (except for gain) do not show any significant change from their values at the start of the measurement. Fig. 13 displays the gain versus HV plots before and after more than 3000 C of charge collection. Ratio of the gains as a function of the HV is also displayed in Fig. 13—bottom.

5. Overall results

Results of all the measurements for all the tubes are organized into a database easily accessible by the collaboration through the internet. In addition to the individual distributions displayed in the figures above, we have also looked at various combinations of the measured quantities. We have

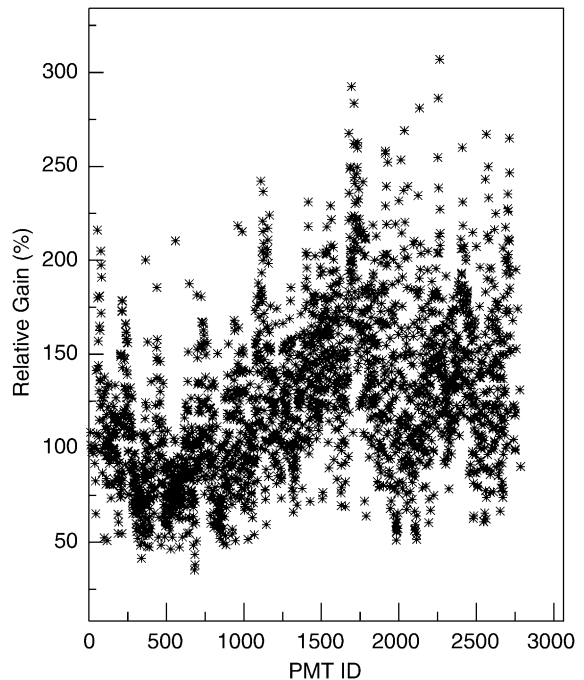


Fig. 14. Relative gains as a function of PMT IDs. PMT IDs roughly correspond to the production time.

not seen any correlation in these scatter plots. We also studied the time variations in the production by plotting the quantities as a function of the serial number. Serial numbers roughly correspond to production time. Only the relative gain results show some variation as a function of the production time. The manufacturer seems to have delivered PMTs with higher combined gain and quantum efficiency at later times (Fig. 14). To see if there is any time-dependent systematic effect in our measurements, we have repeated the measurements for the initial 300 tubes after testing about 1500 tubes. The differences are within the statistical fluctuations. We also remeasured the absolute gain of the reference tube at different stages. It is also constant within the statistical fluctuations.

6. Discussion and conclusion

Among the 2000 tubes tested for the CMS-HF Forward Calorimeter, we have rejected only 20 tubes mainly for high dark current. All the other

PMTs have the same timing characteristics and their dark currents are well below the limits set by the HF requirements. Lifetime measurements performed on two PMTs show that these tubes may perform within their specifications for much longer than the accumulated charge required by the HF Forward Calorimeter.

All the PMTs are sorted according to their relative gains so that the PMTs in a group have the same relative gain within a few percent. To provide uniform gains over similar locations in each wedge, PMTs with almost the same relative gain should be installed in the readout boxes corresponding to those wedges.

Acknowledgements

We would like to thank our colleagues from CMS, in particular Peter Bruecken, Quarknet students from Cedar Rapids and Davenport High School, John Elias, Jim Freeman, Dan Green, Mithat Kaya, Claudio Rivetta, and Andris Skuja

for their encouragement and support. We have appreciated the efforts of the manufacturer Hamamatsu, for producing such high quality PMTs. This work was supported by the US Department of Energy (DE-FG02-91ER-40664), NSF (NSF-INT-98-20258), Turkish Atomic Energy Commission (TAEK) and the Scientific and Technical Research Council of Turkey (TÜBİTAK). We also thank the University of Iowa, Office of Vice-President of research and Bogazici University Scientific and Technological Research Fund (04B301) for their support.

References

- [1] U. Akgun, W. Anderson, A.S. Ayan, E. Gülmez, M. Miller, Y. Onel, I. Schmidt, D. Winn, IEEE Trans. Nucl. Sci. NS-51 (2004) 1909.
- [2] U. Akgun et al., Tests of the CMS-HF Light Guide System at the University of Iowa PMT Test Station, CMS Internal Note: IN 2002/029, 2002, http://cmsdoc.cern.ch/documents/02/in02_029.pdf.